### **CONFERENCE PRE-PRINT**

# DIMENSIONAL ISOTOPE SCALING OF HEAT AND PARTICLE TRANSPORT BETWEEN JET DEUTERIUM AND TRITIUM L-MODE PLASMAS

T. TALA, A. JÄRVINEN, A. SALMI, J. KARHUNEN, A. KIRJASUO

VTT, P.O. Box 1000, FI-02044 VTT, Espoo, Finland

Email: tuomas.tala@vtt.fi

A. MARIANI, P. MANTICA

Istituto di Fisica del Plasma, via Cozzi 53, Milano, Italy

F. ALBERT

Aalto University, Espoo, Finland

I. CARVALHO

ITER Organization, Route de Vinon-sur-Verdon, CS 90 046, 13067 St Paul Lez Durance Cedex, France

A. CHOMICZEWSKA, W. GROMELSKI

IPPLM, Warsaw, Poland

N. HAWKES, M. LENNHOLM, D. KING, C. MAGGI, M. MASLOV, S. MENMUIR, R. SHARMA, H. SUN UKAEA, Culham Campus, Abingdon, OX14 3DB, UK

E. DELABIE, B. LOMANOWSKI

Oak Ridge National Laboratory, Oak Ridge, Tennessee, US

J. FERREIRA

Instituto de Plasmas e Fusão Nuclear, Universidade de Lisboa, Lisboa, Portugal

E. SOLANO

CIEMAT, Madrid, Spain

E. VIEZZER

University of Sevilla, Sevilla, Spain

JET contributors\* and WPTE contributors\*\*

\*See the authorlist of C. Maggi et al., Nucl. Fusion 64, 112012 (2024)

(https://doi.org/10.1088/1741-4326/ad3e16)

\*\*See the authorlist of E. Joffrin et al., Nuclear Fusion 64, 112019 (2024)

(https://doi.org/10.1088/1741-4326/ad2be)

#### **Abstract**

The dimensionally matched deuterium-tritium pulse pair showed 13-16% improvement in the energy confinement time in favour of the tritium pulse. This favourable isotope scaling can be seen clearly in the effective diffusion coefficients throughout the radius. The isotope scaling originates dominantly from the electron heat transport channel and the edge part of the plasma. The phase and amplitude profiles in the response to the gas puff modulation robustly show that there is no isotope scaling in the particle transport channel in the core plasma at  $\rho_{tor} \leq 0.95$ .

Local linear and non-linear GENE simulations are qualitatively consistent with the experimental observations at the edge plasma – the modelling at  $\rho_{tor}=0.95$  predicts a significant favourable isotope scaling for tritium over deuterium for the deuterium-tritium experimental pulse pair. The simulations also that the isotope scaling is stronger at fixed edge density, which is the way the dimensional isotope scaling experiment is conducted. In the dimensionless isotope scaling experiment where density is scaled down as  $\propto 1/m_i$ , GENE shows a much weaker isotope scaling at  $\rho_{tor}=0.95$  especially in the electron heat transport channel.

#### 1. INTRODUCTION

The JET tokamak has the unique capability to perform experiments with tritium (1). Recently, a positive mass dependence of global confinement (sum of core and pedestal) in favour of tritium is reported in the JET type I ELMy H-mode plasmas (2) and in the pedestal (3). While there is no universal mass dependence between deuterium and tritium in the core part of the plasma in JET H-mode plasmas, it may well be that the isotope scaling in the core region in the H-mode plasmas is significantly different from that in L-mode. In L-mode plasmas, by performing a dimensionless match including the isotope mass between the deuterium and tritium plasmas, a  $\sim$ 25% improvement in global confinement and local transport was found (4). Five possible candidates were identified to explain the unexpectedly strong isotope scaling reported in (4); 1) small differences ( $\leq$  10%) in matching the dimensionless parameters in that dimensionless deuterium versus tritium pair, 2) most of the favourable isotope scaling for Tritium would be originating from the edge part of the plasma at  $\rho_{\rm tor} \approx$  0.8–0.95, 3) the electron modes, like ETG, would be stronger than expected, 4) the approximation in not having scaled the electron mass by 50% would have a larger than expected impact on confinement and 5) there would be other differences between these dimensionless discharges, such as the significant  $P_{ei}$  term.

The goal of this paper is to verify the magnitude of isotope mass scaling further in JET L-mode plasmas, and in particular to answer to those 5) open related questions posed in previous paragraph. The emphasis in this paper is put on analysing and modelling of a dimensionally "engineering" matched deuterium tritium pulse pair. Each of the dimensionally matched D versus T pulses have gas puff modulation performed for accurate particle transport and neutral fuelling analysis. The gyro-kinetic GENE simulations are extended up to  $\rho_{tor}=0.95$  to understand better if significant fraction of the origin of the isotope scaling arises from the L-mode plasma edge. The isotope dependence in JET plasmas with internal transport barriers is reported in (5).

### 2. ISOTOPE MASS SCALING BETWEEN THE JET DIMENSIONALLY MATCHED DEUTERIUM TRITIUM PAIR

The dimensional isotope identity experiment between deuterium  $n_D/(n_H+n_D+n_T)=0.95$  and tritium  $n_T/(n_H+n_D+n_T)=0.98$  plasma is illustrated in figure 1. All the engineering parameters  $(I_p,B_t,n_e,P_{nbi})$  are the same between the two dimensionally matched pulses. Gas puff modulation technique, seen on the third panel from top, was exploited here as the tool to study the electron particle transport and edge neutral fuelling, and to quantify more precisely the isotope scaling in the electron particle transport channel. There are no neo-classical tearing modes or other MHD instabilities, except sawtooth, present in this deuterium-tritium pair as reported in detail in paper (6). This dimensionally matched pair exhibited higher plasma radiation and increased Ni and W impurity content in tritium plasmas compared to D plasmas, giving rise to a possibility that isotope mass effect may contribute to enhanced impurity retention and radiation in Tritium plasmas (6). Ni and W were identified as the main core radiators, with  $Z_{eff}=1.5-1.65$ .

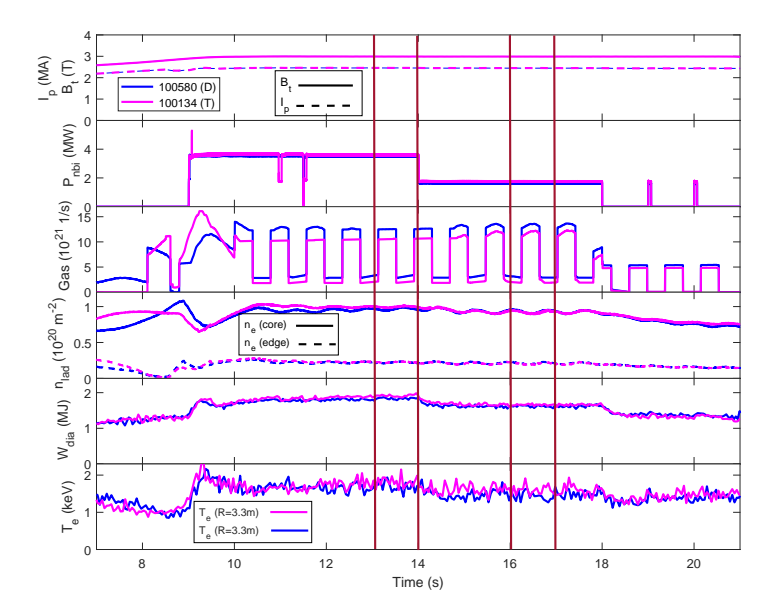


FIG. 1. Key time traces of the deuterium (blue, #100580) and tritium (magenta, #100134) discharges. The four vertical bars indicate the times for averaging two profiles (for figure 2) at two different NBI power levels, at t=13-14s with  $P_{nbi} \approx 5.0$ MW and t=16-17s with  $P_{nbi} \approx 1.7$ MW.

The kinetic profiles and key dimensionless quantities are presented in figure 2. While the density and q-profiles are almost identical, we can observe significantly higher electron temperature, but somewhat lower ion temperature for the tritium pulse. The higher  $T_e$  profile is suggesting a positive isotope scaling for tritium in particular in the electron heat transport channel, which will be quantified later. In contrast to the earlier work with the dimensionless match between deuterium and tritium (4), now  $\rho^*$  is not matched. And due to the isotope scaling favouring the tritium pulse yielding higher  $T_e$ ,  $\nu^*$  is lower for and  $\beta_n$  higher for the tritium discharge.

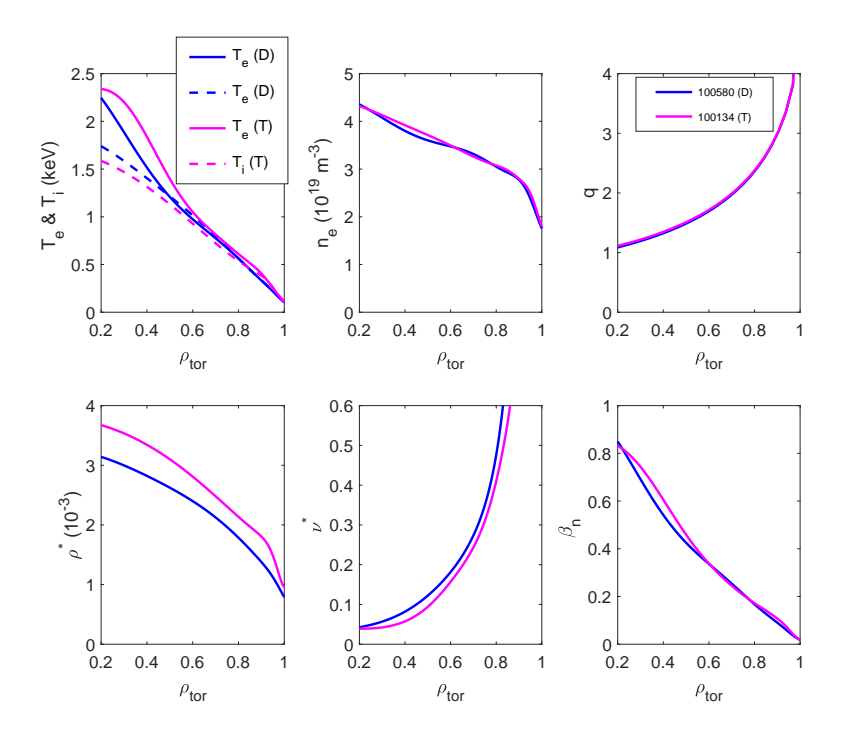


FIG. 2. Ion and electron temperature (top left), electron density (top middle), q-profile (top right),  $\rho^*$  (bottom left),  $\nu^*$  (bottom middle) and  $\beta_n$  (bottom right) profiles for deuterium (blue, #100580) and tritium (magenta, #100134) discharges. The profiles are averaged over the period t=16-17s.

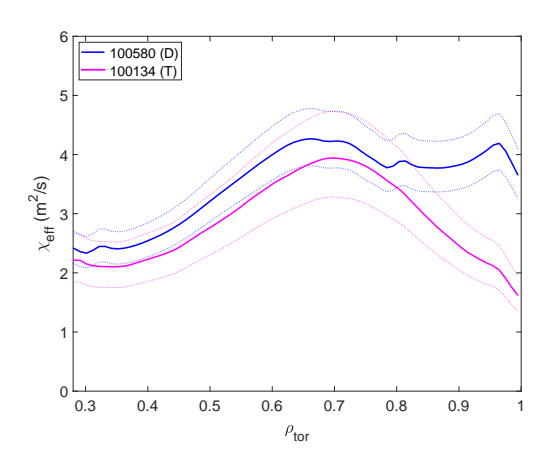
TABLE 1. The comparison of the key 0D quantities for the Deuterium (#100580) and Tritium (#100134) isotope mass scaling pair at the two matched power levels, at  $P_{abs} \approx 3.5 \text{MW}$  and  $P_{abs} \approx 5 \text{MW}$ .

	D: 3.5MW	T: 3.5MW	D: 5MW	T: 5MW
Isotope	D	T	D	T
$B_t$ (T)	2.99	2.99	2.99	2.99
$I_p$ (MA)	2.45	2.45	2.45	2.45
$P_{\rm nbi}$ (MW)	1.61	1.68	3.54	3.54
$P_{\mathrm{OH}}\left(\mathrm{MW}\right)$	2.01	1.73	1.71	1.43
$P_{ m abs}$ (MW)	3.62	3.41	5.25	4.97
$P_{\rm rad}$ (MW)	0.64	0.86	0.62	1.08
$T_e/T_i$	1.05	1.25	1.05	1.20
Mach number	0.12	0.21	0.18	0.31
$\rho^*$ (10 <sup>-3</sup> )	2.5	2.9	2.7	3.2
$ u^*$	0.057	0.045	0.045	0.037
$eta_n$	0.38	0.4	0.46	0.50
$\tau_{E,th}$ (s)	0.27	0.30	0.22	0.26

The energy confinement time  $\tau_{E,th}$  are 0.27s ( $P_{abs} \approx 3.5 \text{MW}$ ) and 0.22s ( $P_{nbi} \approx 5.0 \text{MW}$ ) for the deuterium pulse and correspondingly 0.30s ( $P_{abs} \approx 3.5 \text{MW}$  and 0.26s ( $P_{abs} \approx 5.0 \text{MW}$  for the tritium pulse, yielding 13% and 16% improvement in confinement in favour of the tritium pulse, respectively. Worth noting in table 1 is the lower ohmic heating power, higher

 $T_e/T_i$  ratio, as already discussed in figure 2, and the higher Mach number for the Tritium discharge. The higher ohmic heating power and the higher  $T_e/T_i$  ratio originate from the favourable scaling in the electron heat transport channel of the tritium discharge. The higher Mach number in the case of tritium plasma comes simply from the ion sound speed dependence on isotope mass (at the same NBI torque injection).

The local power and particle balances, heat and particle fluxes and the effective heat and particle diffusion coefficients are calculated with TRANSP and JINTRAC. In order to eliminate the possible effect of the electron-ion heat exchange term, we use the so-called effective one-fluid heat diffusion coefficient  $\chi_{eff}$  defined as  $\chi_{eff} = (q_e + q_i)/(n_e \nabla T_e + n_i \nabla T_i)$ . The effective one-fluid diffusion coefficients at  $P_{abs} = 3.5 \text{MW}$  including the error bar estimates are shown in figure 3 (left frame). Consistently with the global energy confinement in table 1, the effective one-fluid diffusion coefficients show the positive isotope scaling favouring the tritium plasma, in particular toward the edge region of the plasma is well outside the error bars. Decomposition of the effective one-fluid diffusion coefficients into ion, electron and particle transport channels reveals that the confinement improvement in tritium plasma originates dominantly from the electron heat transport channel. This is illustrated in figure 3 (right frame).



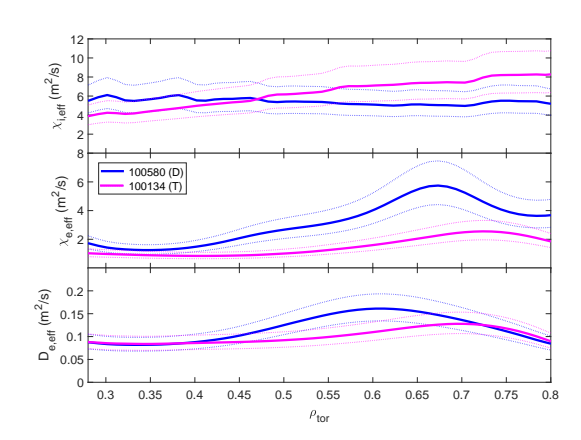


FIG. 3. Effective one-fluid diffusion coefficients for the deuterium discharge (blue, #100580) and the tritium discharge (magenta, #100134) at  $P_{abs}=3.5 \mathrm{MW}$  (left panel) and the corresponding effective ion, electron, and particle diffusion coefficients (right panel), respectively. The dotted lines show the error bars of the estimates.

# 3. ISOTOPE SCALING OF PARTICLE TRANSPORT AND NEUTRAL FUELLING IN JET DEUTERIUM VERSUS TRITIUM L-MODE PLASMAS

Thanks to the gas puff modulation we can study the particle transport in more detail by looking into the dynamic response of the modulated density signal. The JET density profile reflectometry has the sub-ms time resolution (7) needed for this. The density response to gas puff modulation is almost identical between the deuterium and tritium discharges as illustrated in figure 4. Featuring identical phase profiles between the deuterium and tritium plasmas in figure 4 is a strong evidence for the same particle transport between the two isotopes. The slightly higher amplitude profile in deuterium plasma is a consequence of the higher gas puff modulation amplitude needed to achieve the same steady-state density as shown in figure 1 (third panel from above). The particle transport coefficients, shown in figure 5, are calculated using the density modulation methodology according to reference (8). The same particle transport coefficients confirm further that there is no isotope scaling observed in the particle transport channel, at least  $\rho_{tor} < 0.95$ , in these JET L-mode plasmas.

The EDGE2D-EIRENE simulations to study the isotope dependence of neutral fuelling indicate about 15% better neutral penetration across the separatrix in deuterium plasma at comparable separatrix densities. These simulations were calibrated against the mid-plane profiles, target Langmuir probe measurements, and the main chamber deuterium spectroscopy (no drifts) as in paper (9). The ionisation profiles are correspondingly higher in the deuterium plasma. Therefore, the observed improved fuelling in deuterium does not explain the favorable isotope mass scaling for tritium plasma, rather the opposite takes place, making the isotope scaling due to transport effectively larger in the edge part of plasma at  $\rho_{tor} \geq 0.95$ . To quantify better the isotope scaling of neutral fuelling, further simulations are needed.

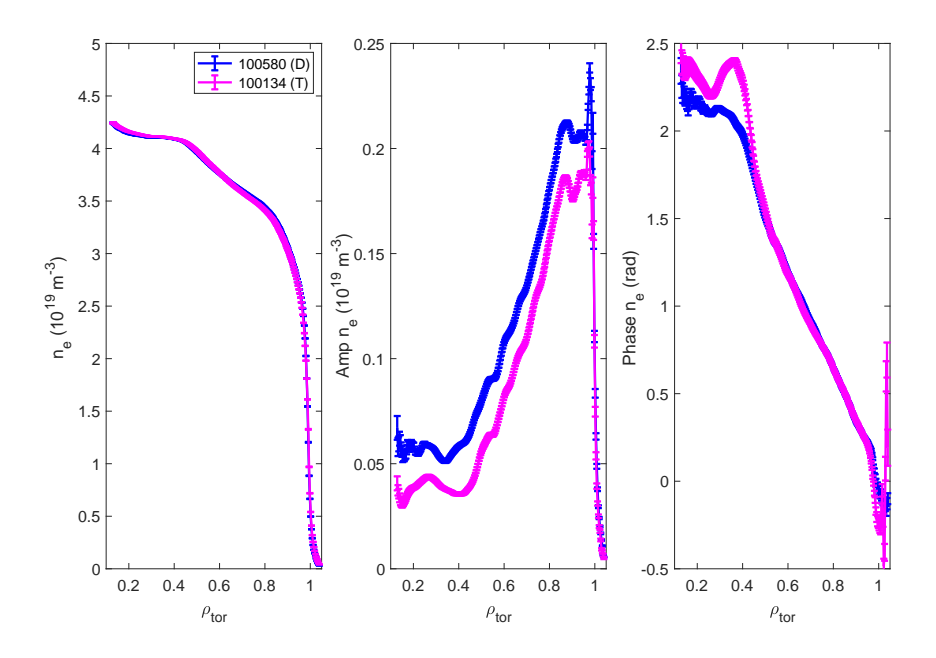


FIG. 4. The steady-state density (left), amplitude (middle) and phase (right) profiles with error estimates for the dimensionally matched isotope scaling discharges of deuterium (blue, #100580) and tritium (magenta, #100134). The data are taken at t=15-18s.

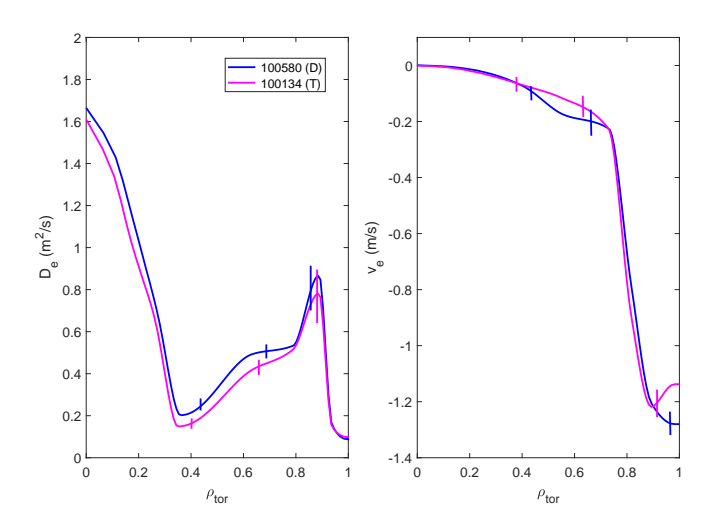


FIG. 5. The particle diffusion (left) and convection (right) profiles for deuterium (blue, #100580) and tritium (magenta, #100134) for the dimensionally matched isotope scaling discharges with data as in figure 4.

# 4. GENE SIMULATIONS OF THE JET EDGE L-MODE PLASMAS TO QUANTIFY THE EDGE CONTRIBUTION TO OVERALL ISOTOPE SCALING

In order to understand possible reasons for the large isotope scaling between deuterium and tritium, local linear and non-linear gyrokinetic flux-tube GENE simulations have been performed in the plasma edge region at  $\rho_{tor}=0.95$ . Non-linear GENE simulations of the tritium pulse (#100143) are compared with "numerical D" and "numerical H" cases with all data from the tritium pulse except the isotope mass set from A=3 to A=2 or A=1, respectively. Impurities were neglected, because of the high computational cost of these simulations at the plasma edge. The  $E\times B$  shearing (computed from full radial electric field) and parallel flow shear were considered consistently in the nonlinear simulations. The GENE nonlinear spectra are shown in Fig. 6 (a) and (b), compared with the corresponding linear growth rates, for the simulations with reference

experimental values (a) and with setting  $T_i = T_e$ ,  $a/L_{Ti} = a/L_{Te}$ . The latter choice reflects the strong electron-ion coupling in the L-mode edge, that could be consistent with having  $T_i = T_e$  at  $\rho_{tor} = 0.95$  within the experimental  $T_i$  error bars. GENE shows a strong edge isotope effect, both in the ion and electron heat fluxes, at  $\rho_{tor} = 0.95$ , much stronger than at  $\rho_{tor} = 0.6$  (see the following). In particular, at reference parameters, one has  $q_i[gB](T) = q_i[gB](D)$ -53% and  $q_i[gB](D) = q_i[gB](H)$ -40%, while when imposing  $T_i = T_e$  (from here on, when writing  $T_i = T_e$ , also  $a/L_{Ti} = a/L_{Te}$  is implied) one has  $q_i[gB](T) = q_i[gB](D)$ -30% and  $q_i[gB](D) = q_i[gB](H)$ -45%. Similar ratios hold for the electron heat fluxes. Here,  $q[gB] = qe^2a^2B_0^2/\sqrt{m_i}n_eT_e^{5/2}$  indicates the heat flux in gyro-Bohm units. The linear frequencies (not shown for brevity) indicate a continuous TEM/ITG branch which rotates in the electron diamagnetic direction for the relevant wave numbers contributing to the nonlinear fluxes. The growth rates also indicate an anti-gB behaviour, consistent with the nonlinear results.

It is difficult to quantify the linear isotope effect by just looking at Fig. 6. To do that, a different approach must be

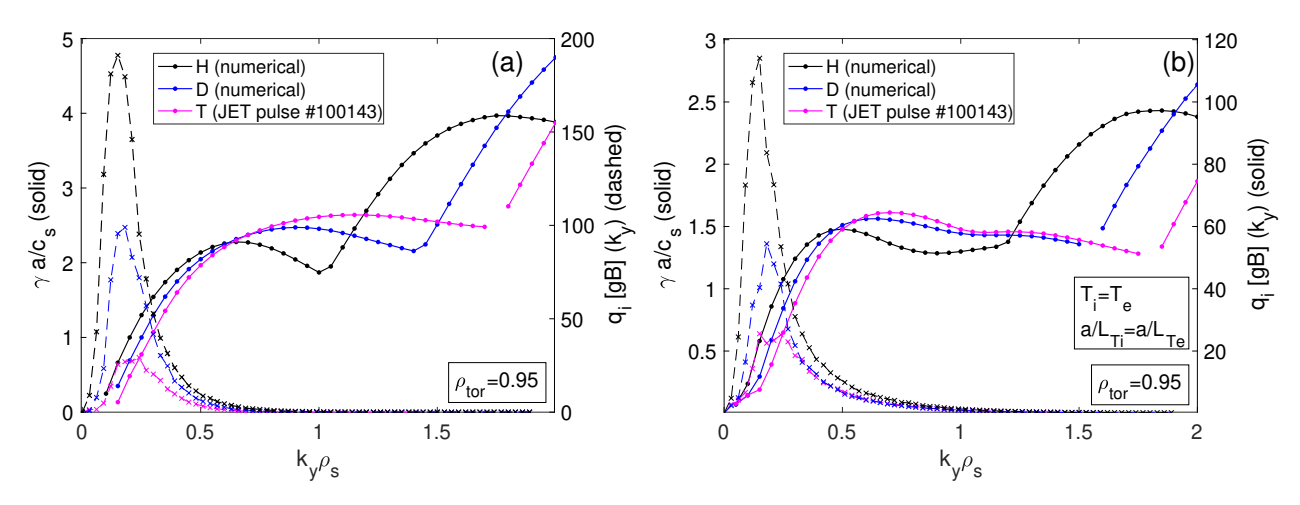
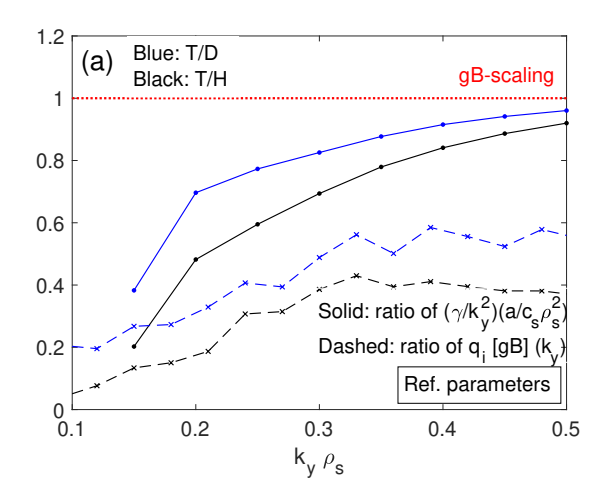


FIG. 6. Linear spectra of the growth rate  $\gamma$  (solid), compared with the nonlinear spectra of the ion heat flux  $q_i$ (dashed) in gyro-Bohm units.  $\gamma$  is normalized with  $c_s/a$ , where  $c_s=\sqrt{T_e/m_i}$  is the sound speed and  $a=\sqrt{\Phi_{edge}/\pi B_0}$  provides a measure of the minor radius. Finally, the binormal wavenumber  $k_y$  is normalized with the inverse of the sound Larmor radius  $\rho_s=c_s/\Omega_i$ . (a) case with reference parameters; (b)  $T_i=T_e$ .

followed. In Fig. 7 (a) and (b), the nonlinear ratios of  $q_i[gB]$  for different isotope pairs (T/D, T/H) are compared with the linear ratios of  $\gamma/k_y^2$  in  $c_s \rho_s^2/a$  units.  $\gamma/k_y^2$  is a rough estimate of the nonlinear saturation value of the electrostatic potential  $|\phi^2| \sim \gamma/\langle k_\perp^2 \rangle$ , that is obtained following a simple mixing length rule. Therefore, since both  $|\phi^2|$  should scale as  $\sqrt{m_i}$  when supposing gyro-Bohm scaling and  $c_s \rho_s^2/a \propto \sqrt{m_i}$ , their ratio should be independent of the isotope mass if the transport is gyro-Bohm. Then, assuming that the nonlinear phase shifts between fluctuating quantities remain sufficiently similar to the linear ones, this ratio can be used as a 'quasi-linear estimate' of the isotope effect. This could then be compared with the nonlinear isotope effect that is computed from the heat fluxes. Figures 7 (a) and (b) show that the 'quasi-linear' isotope effect is similar for the case with reference parameters and the one with  $T_i = T_e$ , while the 'nonlinear' isotope effect is larger for the case with reference parameters. It follows that a quasi-linear model seems able to capture the anti-gyro-Bohm physics for the  $T_i = T_e$  case, while for the other case an additional purely nonlinear physics is at play. To mimic what is done instead when comparing dimensionless identity pulses with different isotopes, where the density changes between the pulses, a numerical experiment was made with GENE considering the assumption  $T_i = T_e$ , which is shown in Fig. 8. Here, the results obtained by only changing the main isotope mass (solid) are compared with those obtained by multiplying n by 2/3 when moving from T to D, or halving it when moving from T to H (dashed). An additional H case is added, where the density is divided by 3 instead of 2 when moving from T to H (red). One observes that the 'direct' isotope effect (solid) basically recovers the 'true' isotope effect which also takes into account the change of density (dashed), except for the H-D comparison in the electron channel, where the 'true' isotope effect is negligible compared to the 'direct' one.

These edge results ( $\rho_{tor}=0.95$ ) are compared with those obtained close to mid-radius ( $\rho_{tor}=0.6$ ) in Ref. (4). The missing H simulations are new and they have been performed for completeness. Remark: at the edge the T pulse #100143 is the reference, with D and H numerical cases, while in the core the D pulse #96092 is the reference, with the H and T numerical cases. The results are shown in Fig. 9. Here, the ratio of heat fluxes in gyro-Bohm units for different isotope pairs (T/D or T/H) is shown, considering three cases:  $\rho_{tor}=0.6$  (solid),  $\rho_{tor}=0.95$  (dashed), and  $\rho_{tor}=0.95$  with  $T_i=T_e$  (dotted). The main result is that the isotope effect is much larger (> twice larger when considering the reference parameters at the edge, smaller difference when considering  $T_i=T_e$  at the edge) compared to mid-radius. Therefore, it could be possible that the large edge isotope effect, through the local non-stiffness of the temperature profiles, could impact the core kinetic profiles and



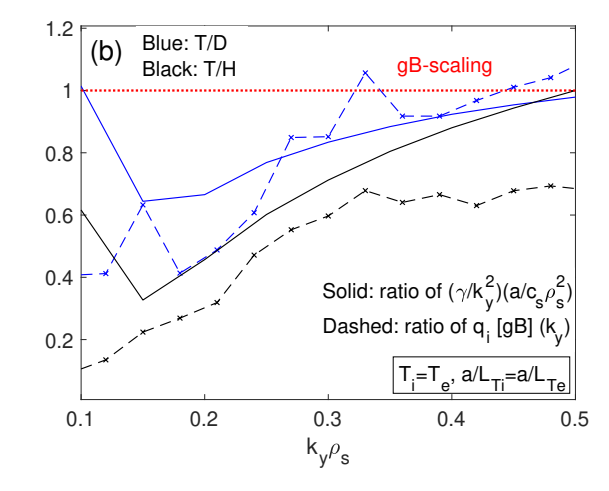
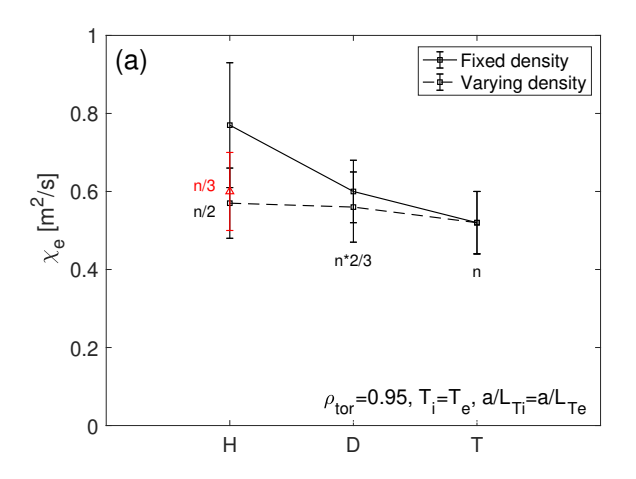


FIG. 7. Spectra of the linear ratios (solid) of  $(\gamma/k_y^2)(a/c_s\rho_s^2)$  for different isotope pairs (T/D: blue; T/H: black), compared with the nonlinear ratios of  $q_i$  [gB] for the same isotope pairs. The red line indicates a pure gyro-Bohm scaling. All the values below the red line indicate an anti-gyro-Bohm scaling. (a) case with reference parameters; (b)  $T_i = T_e$ .



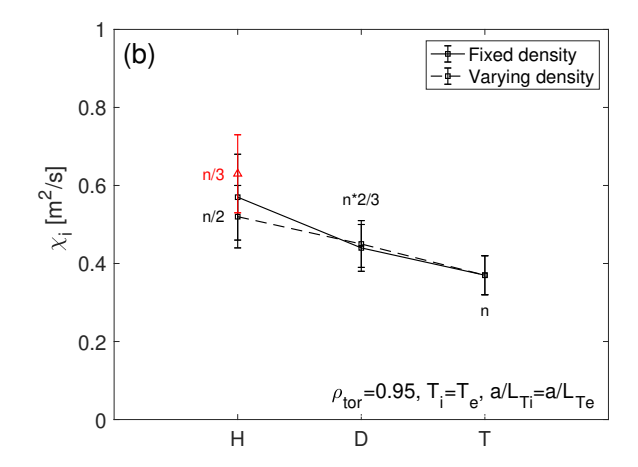


FIG. 8. Heat conductivities  $\chi_e$  (a) and  $\chi_i$  (b) vs main ion isotope, assuming  $T_i = T_e$ . Solid: keeping density fixed; dashed: varying density compared with the reference T case. Red: additional H simulation with n(H) = n(T)/3.

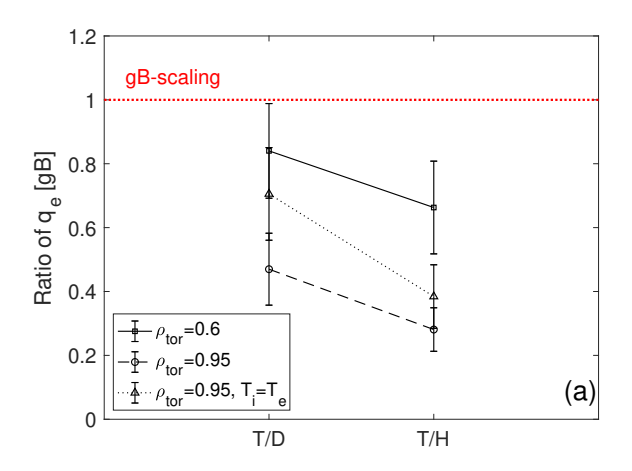
explain the experimental gain of performance with higher mass isotopes.

Finally, work is underway to match the total experimental heat flux  $q_{tot}=q_e+q_i$  and the  $q_e/q_i$  ratio  $\rho_{tor}=0.95$  with GENE. The experimental reference parameters allow one to match  $q_{tot}$ , but with an opposite  $q_i/q_e$  ratio. However, considering  $T_i=T_e, a/L_{Ti}=a/L_{Te}=a/L_{Te}.$  Within experimental error bars, it is possible to get close to both electron and ion experimental fluxes.

### 5. CONCLUSIONS

The dimensionally matched deuterium-tritium pulse pair showed 13-16% (depending on the NBI power level) improvement in the energy confinement time in favour of the tritium pulse. This favourable isotope scaling can be seen clearly in the effective diffusion coefficients. Experimentally, the isotope scaling originates dominantly from the electron heat transport channel and the edge part of the plasma. The phase and amplitude profiles in the response to the gas puff modulation robustly show that there is no isotope scaling in the particle transport channel in the core plasma at  $\rho_{tor} \leq 0.95$ .

Local linear and non-linear GENE simulations are qualitatively consistent with the experimental observations at the edge plasma – the modelling at  $\rho_{tor}=0.95$  predicts significant favourable isotope scaling for tritium over deuterium for this experimental pulse pair. The simulations also show that the isotope scaling is stronger at fixed density as is the case with the dimensionally matched isotope scaling experiment and weaker when density is scaled down for lighter isotopes as is done in the dimensionless isotope scaling experiment. This can potentially resolve the past JET observation with no isotope scaling



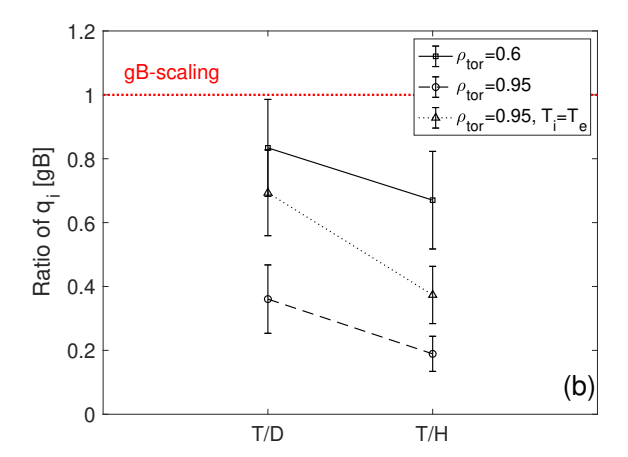


FIG. 9. Radial dependence of the isotope effect. Ratio of electron (a) and ion (b) heat fluxes for different isotope pairs (x axis:T/D,T/H), at different radial positions:  $\rho_{tor}=0.6$  (solid),  $\rho_{tor}=0.95$  (dashed). Additional case:  $\rho_{tor}=0.95$ , with  $T_i=T_e$  (dotted). The red line indicates a pure gyro-Bohm scaling. All the values below the red line indicate an anti-gyro-Bohm scaling.

between H and D reported in the dimensionless hydrogen versus deuterium isotope scaling experiment (10). Further work is still needed for quantitative agreement on heat fluxes between the GENE simulations and experiment for final conclusions from the origin of the significant isotope scaling between the deuterium and tritium plasmas in JET.

### **ACKNOWLEDGEMENTS**

This work has been carried out within the framework of the EUROfusion Consortium, funded by the European Union via the Euratom Research and Training Programme (Grant Agreement No 101052200 EUROfusion). Views and opinions expressed are however those of the authors only and do not necessarily reflect those of the European Union or the European Commission. Neither the European Union nor the European Commission can be held responsible for them.

#### **REFERENCES**

- [1] Maggi C.F. et al., Nucl. Fusion, vol. 63, p. 110201, 2023.
- [2] Schneider P. et al., Nucl. Fusion, vol. 63, p. 112010, 2023.
- [3] Frassinetti L. et al., Nucl. Fusion, vol. 63, p. 112009, 2023.
- [4] Tala T. et al., Nucl. Fusion, vol. 63, p. 112012, 2023.
- $[5] \ \ Maggi \ C.F.\ et\ al.,\ this\ conference,\ p.\ ID\ 2918,\ 2025.$
- [6] Chomiczewska A. et al., Nucl. Fusion, vol. 65, p. 016045, 2025.
- [7] Sirinelli A. et al., Rev. Sci. Instrum., vol. 81, p. 10D939, 2010.
- [8] Salmi A. et al., Plasma Phys. Control. Fusion, vol. 65, p. 055025, 2023.
- [9] Horvath L. et al., Plasma Phys. Control. Fusion, vol. 65, p. 044003, 2023.
- [10] Maggi C.F. et al., Nucl. Fusion, vol. 59, p. 076028, 2019.